Supporting Information

Chakroborty et al. 10.1073/pnas.1108696108

SI Results

Dopamine Fails to Normalize Tumor Blood Vessels in the Absence of Functional Endogenous Dopamine D_2 Receptors. Lewis lung carcinoma (LLC) is a well-characterized mouse tumor which grows in C57BL/6 mice, and dopamine (DA) $D_2^{-/-}$ receptor mice are available only in the C57BL/6 background (1). LLC were transplanted into the flanks of both DA $D_2^{+/+}$ receptor and DA $D_2^{-/-}$ receptor mice. Interestingly, although DA could normalize the morphology of tumor blood vessels and inhibit leakiness of tumor vasculature in LLC-bearing DA $D_2^{+/+}$ receptor mice, it failed to do so in DA D_2 knockout animals (Fig. S2 *A*–*C*). Together these results confirm the involvement of endogenous DA D_2 receptors in controlling tumor blood vessel morphology and leakiness. This effect of DA was observed on day 8 and continued until day 15 (the last day of our experiment) after completion of treatment.

DA Induces Migration of Pericytes by Up-Regulating Angiopoietin 1 Expression in These Cells. Western blot data demonstrated TEK tyrosine kinase endothelial (Tie2) receptors to be present in these pericytes (Fig. S6*A*) (2, 3). Scratching with a 200-μL pipette tip created a wound with a size of 800 ± 75 μm. Complete wound closure with no detectable wound was observed 16 h later in DA-treated and scrambled siRNA + DA-treated cells. In contrast, very prominent wounds were observed in the control and eticlopride + DA-treated cells, and siRNA (50 nM)-mediated angiopoietin 1 (Ang1) silenced human brain vascular pericytes (HBVP) treated with DA after 16 h of wounding (Fig. S6 *B* and *C*). These in vitro wound assay results indicate that DA up-regulates Ang1 expression in HBVP by acting through its D_2 receptors present in these cells and thereby induces migration of these cells (Fig. S6).

DA Inhibits H_2O_2-Induced Permeability in Endothelial Cells. Our results indicated that DA, acting through its D_2 receptors present in human umbilical vein endothelial cells (HUVEC), significantly inhibited H_2O_2-induced permeability in these cells (Fig. S7*A*). This effect was observed 6 h after DA treatment, and it coincided with the time required for DA to induce Krüppel-like factor-2 (KLF2) expression in these cells (Fig. 5 *E* and *F*). However, DA failed to inhibit permeability in KLF2-deficient HUVEC (transfected with a 50-nM concentration of siKLF2 for 48 h, replated on the transwell) challenged with H_2O_2 (Fig. S7*B*). In comparison, DA treatment significantly inhibited H_2O_2-induced permeability in HUVEC when these cells were transfected with scrambled siRNA (Fig. S7*B*). These results suggest that DA can regulate functions of endothelial cells by up-regulating KLF2 expression in these cells.

ERK5 Activation by Stimulation of DA D_2 Receptors Is Associated with Increased Expression of KLF2 in Endothelial Cells. Our results indicate that DA treatment can induce KLF2 expression and phosphorylation of ERK5 in tumor endothelial cells (TEC) collected from PC3 and HT29 tumor-bearing mice (Fig. S8*A*). However, the total ERK5 level remained the same in these treated and untreated control cells (Fig. S8*A*). In contrast, treatment of tumor-bearing mice with the D_2 receptor-specific antagonist eticlopride before DA administration abolished these effects of DA (Fig. S8*A*), indicating that the activation of ERK5 in TEC by DA is mediated specifically through its D_2 receptors present in these cells. In these experiments TEC were isolated and pooled from tumor-bearing mice (4, 5).

To confirm the direct effect of DA on ERK5 activation in endothelial cells, serum- and growth factor-starved HUVEC were treated with DA (1 μM) or a D_2 receptor-specific agonist, quinpirole (1 μM). Serum- and growth factor-starved experimental conditions were selected particularly to exclude the effect of DA on the growth factors present in the serum. Significantly increased phosphorylation of ERK5 was demonstrated in DA- or quinpirole-treated HUVEC, in comparison with untreated controls (Fig. S8*B*), an action that was abolished when these cells were pretreated with the DA D_2 receptor-specific antagonist eticlopride (1 μM) (Fig. S8*B*).

Importantly, DA failed to up-regulate KLF2 expression in HUVEC when these cells were pretreated with 50 nM of ERK5 siRNA (Fig. S8*C*). However, when these cells were transfected with scrambled siRNA, significant up-regulation of KLF2 expression was observed in these cells following DA treatment (Fig. S8*C*). These results indicate that DA mediated-KLF2 up-regulation in endothelial cells occurs through the activation of ERK5.

SI Materials and Methods

Cells and Reagents. PC3, HT29, and LLC cells (ATCC) were cultured in F-12K, McCoy's 5A meduim, and DMEM (ATCC), respectively, supplemented with 10% FBS. Human brain vascular pericytes (HBVP) (ScienCell) were maintained in pericyte medium supplemented with 2% FCS and pericyte growth supplement (ScienCell). HUVEC (Lonza) were maintained in Endothelial Cell Growth Medium (EGM; Lonza) supplemented with various growth factors and 2% FCS (Lonza). For in vitro experiments, HBVP and HUVEC were serum and growth factor starved for 24 h; then the effects of DA and its agonists or antagonists were assessed. DA (for in vitro use), quinpirole, eticlopride, and tert-Butyl hydroperoxide were purchased from Sigma.

Mice and Tumors. Mouse experiments were performed after approval by the Ohio State University Animal Care and Use Committee. Male athymic nude mice (6–8 wk old) (National Cancer Institute) and DA $D_2^{+/+}$ receptor and DA $D_2^{-/-}$ receptor C57BL/6 mice (Jackson Laboratory) were used for the study. The animals were anesthetized with ketamine/xylazine (100 mg/10 mg, i.p.) before implantation of orthotopic PC3 or HT29 cells. For the prostate cancer model, PC3 prostate cancer cells were cultured in F-12K medium and were harvested when the cells reached 70–80% confluency by rinsing with PBS followed by trypsinization with 1% trypsin. Viable cell number was counted by trypan blue exclusion with the aid of a hemacytometer. Briefly, a low midline incision was made through the skin and peritoneum. The urinary bladder and seminal vesicles were exposed and pushed downward so that the two lobes of the dorsal prostate could be clearly visible. PC3 cells (1.0×10^5) suspended in PBS were injected into the exposed right lobe of the prostate in a volume of 50 μL. The wounds were closed by sutures. The outer incision was closed in two layers, one in the abdominal wall muscle and one in the skin (6). Approximately 45 d after tumor implantation, the abdomen was reopened surgically to detect tumors in the prostate and then was closed. To develop an s.c. model of prostate cancer, 2×10^6 PC3 cells in 0.2 mL PBS were injected s.c. into the right flanks of mice (7).

The orthotopic colon cancer model was developed by exteriorizing the cecum through a small abdominal incision. Then 1×10^6 HT29 cells in 50 μL medium were injected into the cecal wall from the serosal side with a 30-gauge needle. The cecum was returned to the abdominal cavity, and the wound was closed in

one layer. Approximately 60 d after tumor implantation, the abdomens were reopened surgically to detect tumors in the cecum and then were closed (8). Animals with HT29 tumors of similar size in the cecum were divided randomly into control and treatment groups. Also, 1×10^6 HT-29 cells suspended in 100 μL of sterile medium were implanted s.c. into the right flank of nude mice (9).

LLC cultured in DMEM supplemented with 10% FBS were harvested from subconfluent cultures by trypsinization (0.01% trypsin, 5 mM EDTA). Cells were washed and resuspended in PBS. Then 200 μL of resuspended cells (adjusted to a final concentration of 1×10^7 cells/mL) was injected s.c. into the right flank of DA $D_2^{+/+}$ receptor and DA $D_2^{-/-}$ receptor C57BL/6 mice (1).

Drugs and Treatment. DA (American Reagent Laboratories) was administered i.p. at a dose of 50 mg/kg once daily for 7 consecutive days (4, 5, 10, 11). This dose of dopamine corresponds to ~5% of the LD_{50} in mice (12). The normal plasma DA level in mice is 1.5 ± 0.01 pmol/mL, and this i.p. dose of DA raises the plasma DA level in mice to 1.2 ± 0.01 nmol/mL 1 min after administration (5). There is a nonsignificant rise in blood pressure after administration of this dose of DA, but blood pressure returns to the normal basal level within 15 min after i.p. injection. Quinpirole (Sigma) was administered i.p. at a dose of 10 mg/kg once daily for 7 consecutive days (10). Eticlopride (Sigma) was administered i.p. at a dose of 10 mg/kg before treatment with DA (10, 11). 5-Fluorouracil (5-FU) (APP Pharmaceuticals) was administered i.p. either as a single dose of 20 mg/kg in experiments to determine the concentration of 5-FU in tumor tissues or at a dose of 20 mg/kg once daily for 5 consective days (4).

Measurement of Tumor Volume. Tumor growth was determined by caliper measurement of the largest diameter and its perpendicular using the formula, Tumor volume (mm^3) = $0.5 \times a \times b^2$, where a is the largest diameter and b is its perpendicular (4).

Blood Vessel Morphology and Permeability. To visualize blood vessels, mice were injected via the tail vein with 100 μL of FITC-labeled *Lycopersicon esculentum* lectin (1 mg/mL in 0.9% NaCl; Vector Laboratories). After 1 h, mice were anesthetized with ketamine/xylazine (100/10 mg/kg i.p.), chests were opened rapidly, and the vasculature was perfused with fixative (1% paraformaldehyde in PBS, pH 7.4, (Sigma-Aldrich) using an 18-gauge cannula inserted into the aorta via an incision in the left ventricle. Blood and fixative were allowed to exit through an opening in the right atrium. Fixed tissues were removed, immersed in fixative for 1 h at 4 °C, rinsed several times with PBS, infiltrated with 30% sucrose, frozen in Optimal Cutting Temperature (OCT) compound (Sakura), and processed for confocal microscopy. Representative images were collected using an Olympus FV1000 confocal scanning microscope, and vessel diameters were measured using National Institutes of Health Image J version 1.44. Vascular leakage was assessed by i.v. injection of 0.1 mL 10 mg/mL FITC-dextran (200,000 kDa) from Sigma. After 30 min mice were anesthetized with ketamine (100 mg/kg i.p.) plus xylazine (10 mg/kg i.p.), followed by perfusion. Sections were collected, fixed, and processed for confocal images (10, 13).

Modified Miles Assay. Evans blue dye (100 μL of a 1% solution in 0.9% NaCl) was injected i.v. into tumor-bearing mice. After 30 min, the animals were killed, the tumor was removed, and Evans blue dye was extracted from the tumor by incubation with formamide for 5 d at room temperature. The absorbance of dye extracted from tumor was measured at 620 nm (14).

Laser Doppler Flowmetry. The noninvasive laser Doppler flowmetry (LDF) technique was used to assess tumor blood perfusion. We used the Periflux System 5010 LDPM Unit (Perimed) and a PF407-1 probe (Perimed). The LDF signal was recorded continuously for 3 min at 15-min intervals for a total period of 45 min, and the perfusion in arbitrary perfusion units (PU) was monitored graphically. To minimize discomfort for the mice, they were allowed to rest, relax, and acclimatize at room temperature; to keep them motionless during the continuous monitoring, they were anesthetized using ketamine/xylazine. The anesthetized mice were placed on a heating pad (37 °C) to prevent hypothermia. During recording, care was taken to position the probe so that respiratory movements did not influence the reading, which was determined by the graphical representation of the PU values (15).

Tissue Hypoxia. To detect tumor tissue hypoxia, 60 mg/kg pimonidazole was injected i.v. 1 h before the tumors were dissected out. The Hypoxyprobe-1 kit (Chemicon) was used to detect pimonidazole-protein adducts in tumors (n = 3 or 4 animals per group). Digital images of the sections were captured by a laser-scanning confocal microscope at 400× magnification (Olympus FV 1000). The total hypoxic area for each section was divided by the cross-sectional area to obtain the proportion of hypoxic area in the tumor (13, 16).

Confocal Microscopy. PC3 prostate tumor, HT 29 colon tumor, and LLC tumor tissue sections were used to determine the maturity of tumor blood vessels. Tissue sections were subjected to immunofluorescence colocalization of CD31 (BD Biosciences) and neural/glial antigen 2 (NG2) proteoglycan (Chemicon); CD31 and regulator of G protein signaling 5 (RGS5) (Santa Cruz); CD31 and α smooth muscle actin (αSMA) (Sigma); CD31 and PDGF receptor β(PDGFRβ) (Abcam); CD31 and DA D_2 receptor (Santa Cruz); and DA D_2 receptor and Ang1 (Santa Cruz). Briefly, tumor sections were preblocked with 10% goat serum at room temperature for 1 h; primary antibodies were added and incubated at 4 °C overnight. The next day sections were washed with PBS, and secondary antibodies (Alexa Fluor 488 and Alexa Fluor 633) (Invitrogen) were added and incubated for 30 min at room temperature. Sections were mounted with Vectashield mounting medium (Vector Labs) with or without DAPI for fluorescence microscopy using an Olympus FV1000 camera. For in vitro studies with endothelial cells, cells were fixed with 4% paraformaldehyde for 5 min before blocking; KLF2 antibody (Abcam) was added, incubated overnight, and then stained with anti-rabbit Alexa Fluor 488 (10, 13).

Assay of DA by HPLC. Tissue samples were weighed and homogenized in 10.2 mL of ice-chilled 0.6 M perchloric acid containing 1.7 mg/mL ethylene glycol tetra acetic acid and 1.1 mg/mL reduced glutathione followed by centrifugation for 15 min at 2,500 × g at 0 °C. Then 1.0 mL of the supernatant was adjusted to pH 8.6 with 6 M potassium hydroxide and was processed to determine the DA concentration after alumina-batch extraction. Then 25 μL of 3 M potassium chloride was added to 200 μL of the 0.2 M perchloric acid eluate and was centrifuged; then 50 μL of the supernatant was injected into the HPLC system. The limit of sensitivity in the supernatant, defined as two times baseline noise, was 0.01 ng/mL for DA. If a concentration was lower than the limit of sensitivity, the concentration of the DA was assigned the value zero (5).

Isolation of Tumor Endothelial Cells. Suspensions of PC3 and HT29 tumor cells were made by passage of viable tissue through sieve and treatment with collagenase and DNase. The cells were washed, red blood cells were lysed with PharMLyse (BD PharMingen), and cell pellets were resuspended in FACS buffer (1× PBS + 1% BSA), preblocked with an Fc block (CD16/32), and then incubated with phycoerythrin-conjugated anti-VEGF re-

ceptor 2 (1:100), CD31 (1:100), and CD34 (1:100). Tumor endothelial cells were collected by FACS (4, 5).

Western Blot Analysis. Western blot analyses were performed on HBVP using goat polyclonal antibody against Ang1 and goat polyclonal antibody against DA D_2 receptor and Tie2 (Santa Cruz); on TEC and HUVEC using rabbit polyclonal antibody against KLF2 (Abcam) and goat polyclonal antibody against DA D_2 receptor, and phospho ERK5 and ERK 5 (Invitrogen) (4, 5).

Quantification of 5-FU in Tumor Tissues. A 50-mg aliquot of tumor tissue was mixed with 200 μL ice-cold PBS, and the mixture was homogenized on ice. After spinning down, the supernatant was transferred to a new Eppendorf tube as the tumor tissue extract. 5-FU then was extracted, and its concentration was determined by liquid chromatography electrospray ionization tandem mass spectrometry (17).

siRNA Knockdown of Specific Proteins. HBVP were plated at 50% confluence on six-well plates precoated with poly-L-lysine (2 μg/cm^2. Ang1 siRNA (Santa Cruz) solution was diluted further with transfection medium (Santa Cruz) and mixed with siRNA transfection reagent (Santa Cruz) and culture medium to achieve a final siRNA concentration of 50 nmol/L. Transfected cells were incubated at 37 °C for 48 h. siRNA concentrations were optimized to ensure that they did not affect cell viability (18).

For KLF2 and ERK5 silencing of HUVEC, cells were plated 1 d before transfection in EBM medium. siRNA targeting KLF2 and ERK5 purchased from Dharmacon were diluted using serum-free medium containing DharmaFECT transfection reagent to achieve a final concentration of 50 nmol/L and were incubated for 48 h. The concentrations of siRNAs were optimized to ensure that they did not affect cell viability (19, 20).

Migration Assay. An in vitro wound-healing assay was undertaken to evaluate pericyte migration following DA treatment. HBVP were cultured to near confluence in 24-well plates precoated with poly-L-lysine (2 μg/cm^2) in pericyte medium containing 2% FCS at 37 °C. Cells were serum and growth factor starved for 24 h, and then cell monolayers were wounded by a p200 pipette tip in one direction to create a scratch. The wounded cells were washed with PBS to remove cellular debris. To assess the effect of DA, cells were treated with DA (1 μM) or eticlopride (1 μM) followed by DA and were incubated at 37 °C for 16 h. To assess the role of Ang1 in pericyte migration, HBVP were grown to 50–60% confluency and then were transfected with Ang1 siRNA (50 nM/L) (Santa Cruz) or the nontargeting control siRNA (Santa Cruz) (13) and were incubated at 37 °C until cells reached 100% confluence to form a monolayer before the 200-μL pipet tip was used to create the scratch. Pericyte migration was monitored every 2 h under a phase-contrast microscope for 16 h after initial wounding, at which time no evident wound was observed in DA-treated plates. Wound closure was calculated as the distance covered by cells in relation to the initial distance between the two wound edges and is expressed as a percentage (2, 21).

Measurement of Endothelial Permeability. An in vitro vascular permeability assay kit (Millipore) was used to measure endothelial cell monolayer permeability to high-molecular-mass proteins using 200,000-kDa FITC-dextran. Briefly, HUVEC were seeded onto collagen-precoated cell-culture inserts at a density of 4×10^5cells per insert in a final volume of 250 μL EGM with supplements. The inserts were placed overnight into 24-well plates containing 500 μL medium. Cells were incubated at 37 °C until a monolayer was formed, were starved of serum and growth factors overnight, and then were incubated with DA or eticlopride followed by DA or were left as control. After incubation at 37 °C for 6 h, cells were treated with 200 μM/L tert-Butyl hydroperoxide (Sigma). Then 150 μL FITC-dextran was added to the insert and incubated for 2 h. The insert was removed, and 100 μL medium was collected from the bottom chamber. The fluorescence density of samples was analyzed using a fluorescence plate reader with excitation and emission wavelengths of 485 nm and 535 nm, respectively. To assess the effect of KLF2 silencing on endothelial cell permeability, HUVEC were transfected with 50 nM KLF2 siRNA or scrambled siRNA (Dharmacon). Results are expressed as relative permeability in which the control group was set as one (19).

Statistical Analyses. All data are expressed as mean ± SEM. Differences among groups were evaluated by ANOVA and the unpaired Student's t test or Dunn's multiple comparison tests. $P < 0.05$ was considered significant (4, 5).

1. Berdel WE, et al. (1988) Influence of 1-beta-D-arabinofuranosylcytosine conjugates of lipids on the growth and metastasis of Lewis lung carcinoma. *Cancer Res* 48:826–829.
2. Cai J, Kehoe O, Smith GM, Hykin P, Boulton ME (2008) The angiopoietin/Tie-2 system regulates pericyte survival and recruitment in diabetic retinopathy. *Invest Ophthalmol Vis Sci* 49:2163–2171.
3. Iurlaro M, et al. (2003) Rat aorta-derived mural precursor cells express the Tie2 receptor and respond directly to stimulation by angiopoietins. *J Cell Sci* 116:3635–3643.
4. Sarkar C, Chakroborty D, Chowdhury UR, Dasgupta PS, Basu S (2008) Dopamine increases the efficacy of anticancer drugs in breast and colon cancer preclinical models. *Clin Cancer Res* 14:2502–2510.
5. Chakroborty D, et al. (2004) Depleted dopamine in gastric cancer tissues: Dopamine treatment retards growth of gastric cancer by inhibiting angiogenesis. *Clin Cancer Res* 10:4349–4356.
6. Davies MA, et al. (2002) Adenoviral-mediated expression of MMAC/PTEN inhibits proliferation and metastasis of human prostate cancer cells. *Clin Cancer Res* 8: 1904–1914.
7. Furukawa J, et al. (2010) Antisense oligonucleotide targeting of insulin-like growth factor-1 receptor (IGF-1R) in prostate cancer. *Prostate* 70:206–218.
8. Morikawa K, Walker SM, Jessup JM, Fidler IJ (1988) In vivo selection of highly metastatic cells from surgical specimens of different primary human colon carcinomas implanted into nude mice. *Cancer Res* 48:1943–1948.
9. Reinmuth N, et al. (2002) Blockade of insulin-like growth factor I receptor function inhibits growth and angiogenesis of colon cancer. *Clin Cancer Res* 8:3259–3269.
10. Basu S, et al. (2001) The neurotransmitter dopamine inhibits angiogenesis induced by vascular permeability factor/vascular endothelial growth factor. *Nat Med* 7:569–574.
11. Chakroborty D, et al. (2008) Dopamine regulates endothelial progenitor cell mobilization from mouse bone marrow in tumor vascularization. *J Clin Invest* 118:1380–1389.
12. Zaroslinski JF, et al. (1977) The pharmacology and subacute toxicology of dopamine. *Proc R Soc Med* 70 (Suppl 2):2–6.
13. Hamzah J, et al. (2008) Vascular normalization in Rgs5-deficient tumours promotes immune destruction. *Nature* 453:410–414.
14. Satchi-Fainaro R, et al. (2005) Inhibition of vessel permeability by TNP-470 and its polymer conjugate, caplostatin. *Cancer Cell* 7:251–261.
15. Ley CD, Horsman MR, Kristjansen PE (2007) Early effects of combretastatin-A4 disodium phosphate on tumor perfusion and interstitial fluid pressure. *Neoplasia* 9: 108–112.
16. Samoszuk MK, Walter J, Mechetner E (2004) Improved immunohistochemical method for detecting hypoxia gradients in mouse tissues and tumors. *J Histochem Cytochem* 52:837–839.
17. Remaud G, Boisdron-Celle M, Morel A, Gamelin A (2005) Sensitive MS/MS-liquid chromatography assay for simultaneous determination of tegafur, 5-fluorouracil and 5-fluorodihydrouracil in plasma. *J Chromatogr B Analyt Technol Biomed Life Sci* 824: 153–160.
18. Foubert P, et al. (2008) Coadministration of endothelial and smooth muscle progenitor cells enhances the efficiency of proangiogenic cell-based therapy. *Circ Res* 103:751–760.
19. Lin Z, et al. (2010) Kruppel-like factor 2 regulates endothelial barrier function. *Arterioscler Thromb Vasc Biol* 30:1952–1959.
20. Clark PR, et al. (2011) MEK5 is activated by shear stress, activates ERK5 and induces KLF4 to modulate TNF responses in human dermal microvascular endothelial cells. *Microcirculation* 18:102–117.
21. Oberringer M, Meins C, Bubel M, Pohlemann T (2007) A new in vitro wound model based on the co-culture of human dermal microvascular endothelial cells and human dermal fibroblasts. *Biol Cell* 99:197–207.

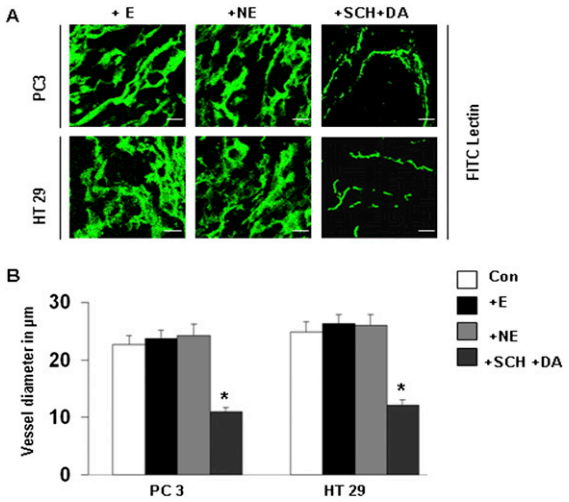

Fig. S1. Epinephrine (E), norepinephrine (NE), and the DA D_1 receptor-specific antagonist SCH 23390 have no effect on the morphology of blood vessels of PC3 and HT29 tumors. (*A*) Confocal microscopy images of vessels perfused with FITC-lectin. (*B*) Mean vessel diameters were quantified from the epinephine-, norepinephrine-, and SCH 23390+DA-treated groups (five fields per tumor). Treatment with epinephrine and norepinephrine cannot normalize tumor vessels, which exhibit dilation and tortuosity similar to that of untreated tumors. Priereatment with SCH 23390 cannot abrogate the effects of DA on the morphology of tumor vessels, which show reduced dilation and tortuosity. Results shown are representative of six separate experiments. *$P < 0.001$. All error bars represent SEM; $n = 15$ for each experimental group. (Scale bars, 50 μm.)

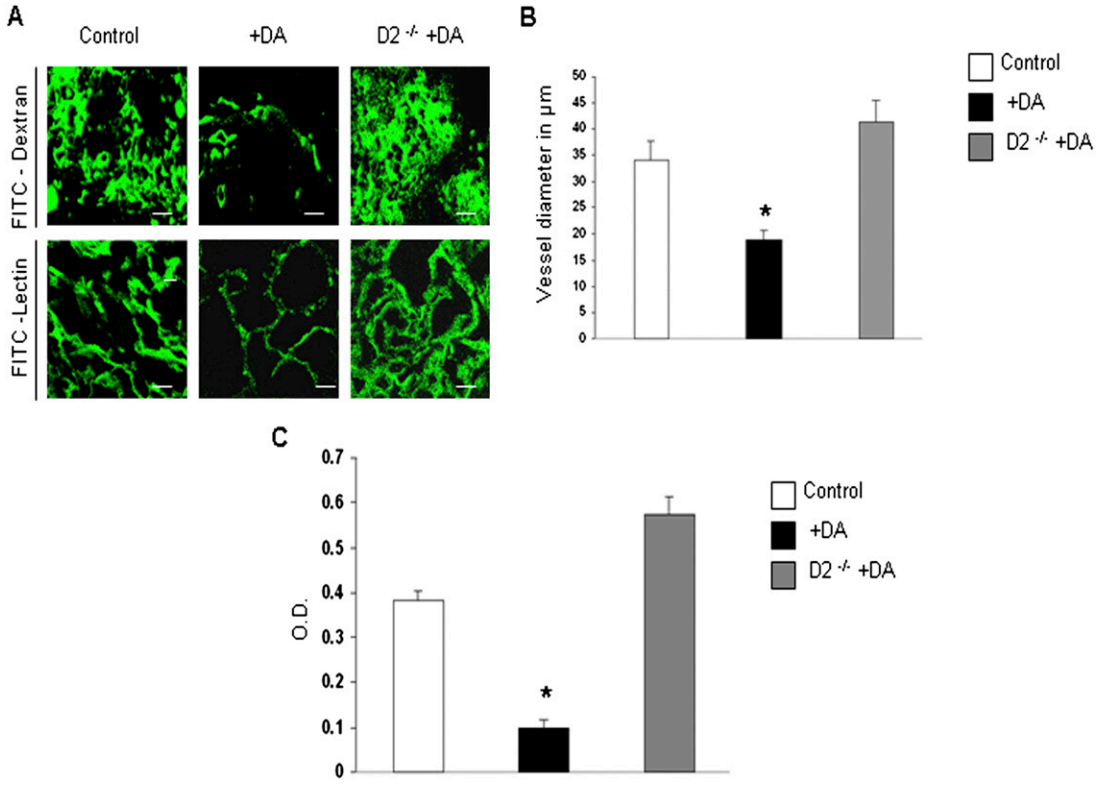

Fig. S2. Role of endogenous DA D_2 receptors on morphology and regulation of leakiness in tumor blood vessels. DA restores normal vessel morphology in LLC tumors transplanted in D_2 receptor$^{+/+}$ C57BL/6 mice but fails to do so in LLC tumors transplanted in D_2 receptor$^{-/-}$ C57BL/6 mice. (*A*) Confocal images of FITC-dextran–perfused vessels and FITC-lectin–perfused vessels in LLC tumors from control, DA-treated D_2 receptor$^{+/+}$, and DA-treated D_2 receptor$^{-/-}$ C57BL/6 mice. Untreated tumor vessels exhibit dilation, tortuosity, and extensive leakiness. In contrast, treatment with DA markedly reduces tumor vessel dilation, tortuosity, and leakiness. However, DA fails to show similar effects in LLC tumors grown in D_2 receptor$^{-/-}$ C57BL/6 mice. (Scale bars, 50 μm.) (*B*) Mean vessel diameters were quantified from control, DA-treated D_2 receptor$^{+/+}$, and DA treated D_2 receptor$^{-/-}$ C57BL/6 mice (five fields per tumor). (*C*) A modified Miles assay shows significantly decreased vessel leakiness in LLC tumors grown in D_2 receptor$^{+/+}$ C57BL/6 mice following DA treatment for 7 d. This effect of DA was not observed when D_2 receptor$^{-/-}$C57BL/6 mice bearing LLC were treated with DA for 7 d. Vascular permeability was assessed colorimetrically from the degree of extravasation of Evans blue dye from tumor vessels. *$P < 0.001$. All error bars represent SEM; $n = 15$ for each experimental group.

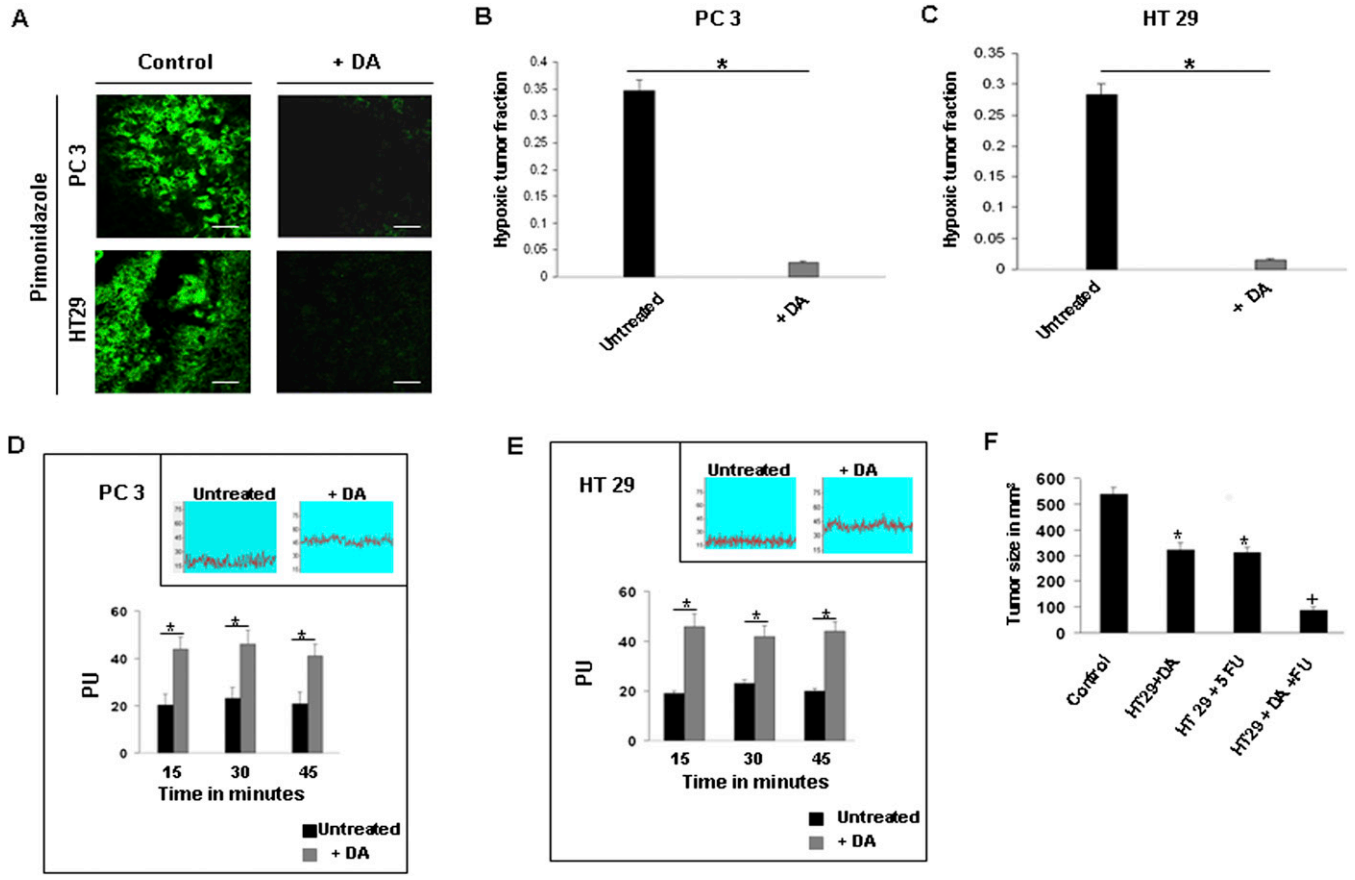

Fig. S3. Dopamine (DA) decreases tumor hypoxia, improves blood flow in PC3 prostate and HT29 colon tumor tissues, and increases concentration of 5-FU in HT29 colon tumor tissues. Detection of hypoxia in tumor tissues of orthotopic PC3 (*A* and *B*) and HT29-bearing (*A* and *C*) mice 10 wk after tumor transplantation. Tumor hypoxia was severe in untreated controls. In contrast, DA treatment significantly decreased hypoxia (*$P < 0.05$). (Scale bars in *A*, 50 μm.) (*D* and *E*) Graphical representations of blood flow measured for 3 min in untreated and DA-treated animals. LDF perfusion at the end of treatment with DA shows that DA treatment significantly increases perfusion in s.c. PC3 (*D*) and HT29 (*E*) tumors in comparison with untreated controls (*$P < 0.005$). Blood flow was measured three times for 3 min at 15-min intervals. (*F*) Treatment of HT29 tumor-bearing mice with DA (50 $mg \cdot kg^{-1} \cdot d^{-1}$ i.p.) for 7 d followed by 5-FU significantly retards tumor size compared with treatment with 5-FU alone, indicating increased efficacy of 5-FU in the DA-pretreated group. *$P < 0.05$; #$P < 0.05$ compared with control and 5-FU -treated groups. All error bars represent SEM; $n = 15$ for each experimental group.

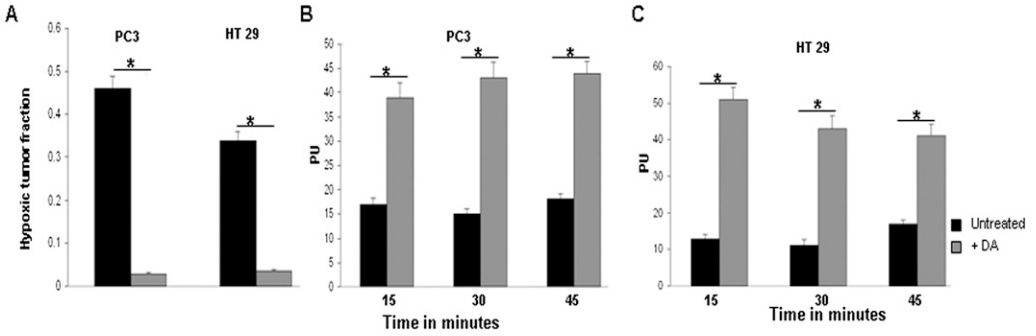

Fig. S4. Effect of DA on tumor hypoxia and blood flow in PC3 and HT 29 tumors 15 d after the start of DA treatment. DA treatment was started on day 1 and stopped on day 7. Even on day 15, DA-treated tumors show significantly reduced hypoxic fraction (*A*) and improved blood flow (*B* and *C*). Results shown are representative of six separate experiments.*$P < 0.05$.

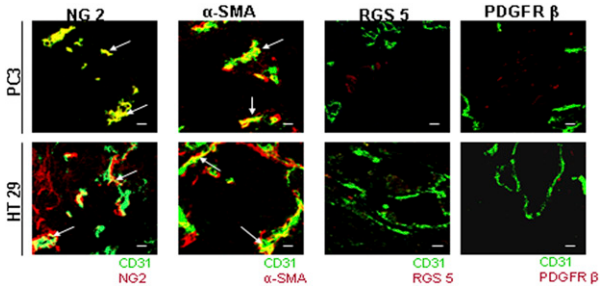

Fig. S5. Treatment with the long-acting dopamine D_2 receptor agonist quinpirole increases the number of mature pericytes in tumor blood vessels. Confocal images of PC3 and HT29 tumor tissues treated with the DA D_2 receptor-specific agonist quinpirole labeled with anti-NG2 (red), anti-α SMA (red), anti-PDGFRβ (red), and anti-RGS5 (red). Endothelial cells were stained with anti-CD 31 (green). A significant decrease is seen in the numbersof $RGS5^+$ and $PDGFR\beta^+$ pericytes in quinpirole-treated tumor blood vessels, and a significant increase is seen in the number of $NG2^+$ and αSMA^+ pericytes in tumor blood vessels. For these images a 40× objective was used. Results shown are representative of six separate experiments. (Scale bars, 20 μm.)

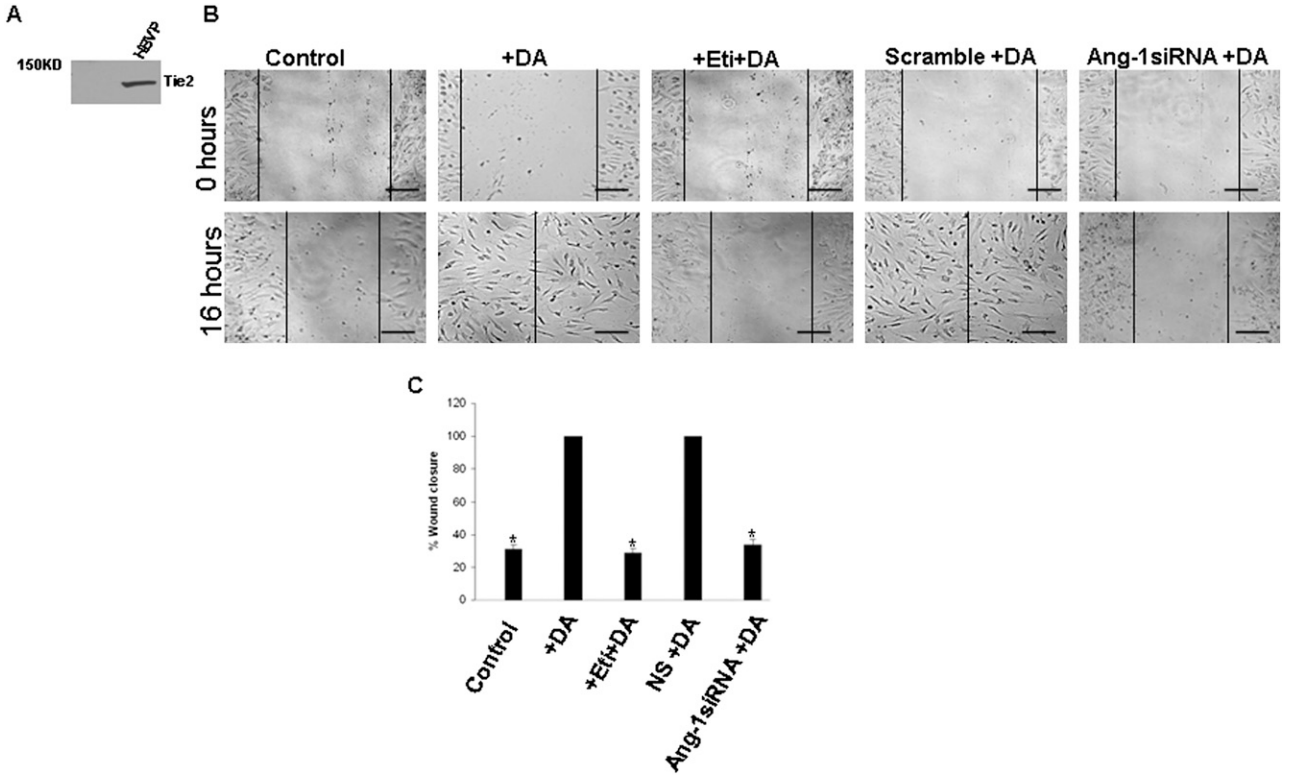

Fig. S6. Effect of DA on pericyte migration. (*A*) Western blot analysis for the detection of the Tie 2 receptor in HBVP. (*B*) Phase-contrast microphotographs of the wound area in the HBVP monolayer just after and 16 h after wounding. HBVP express Tie 2 under standard culture conditions. DA treatment (1 μM) promotes complete wound closure in 16 h. This effect is lost when cells are pretreated with the DA D_2 receptor-specific antagonist eticlopride (1 μM). A prominent wound is seen 16 h after DA treatment in Ang1 siRNA-transfected HBVP, whereas complete wound closure is observed 16 h after DA treatment in HBVP transfected with nonspecific control siRNA. (Scale bars, 200 μm.) (*C*) Wound closure was calculated as the distance covered by cells in relation to the initial wound distance at 0 h and is expressed as a percentage of the initial distance at 0 h. $^*P < 0.05$. All error bars represent SEM. Results shown are representative of six separate experiments.

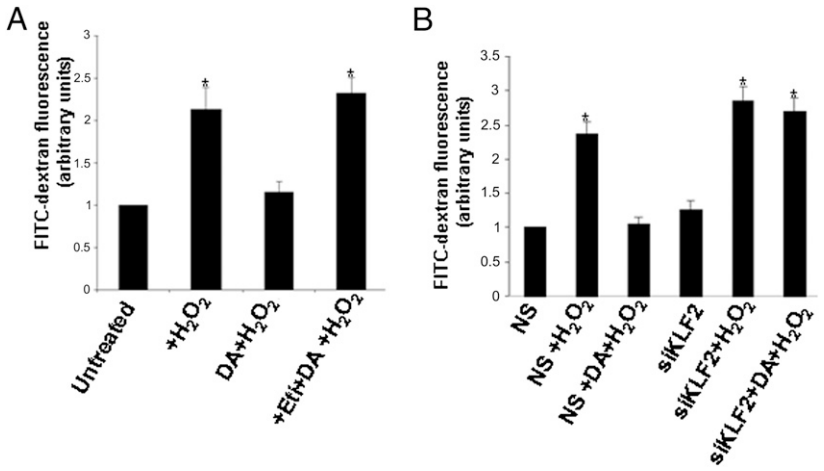

Fig. S7. Direct effect of DA on endothelial leakage in HUVEC. (*A*) DA reduces endothelial cell permeability in HUVEC in response to H_2O_2 (200 μmol/L). Abrogation of DA-induced reduction of endothelial cell permeability by eticlopride (a DA D_2 receptor-specific antagonist) indicates the involvement of DA D_2 receptors in this process. (*B*) DA was unable to reduce endothelial cell permeability in HUVEC transfected with KLF2 siRNA. DA reduces cell permeability in HUVEC transfected with nontargeting control siRNA that also showed increased permeability in response to H_2O_2. Results shown are representative of three independent experiments. $*P < 0.05$. All error bars represent SEM.

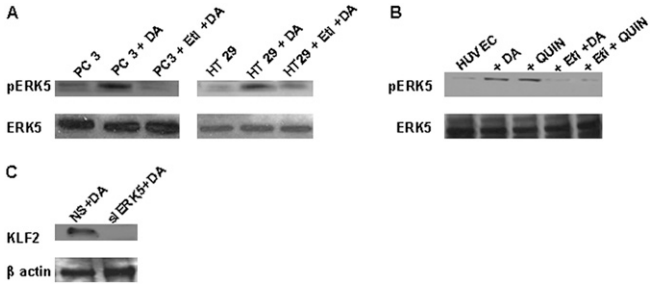

Fig. S8. DA treatment can up-regulate the phosphorylation of ERK5. Phosphorylation of ERK5 was up-regulated in TEC isolated from PC3 and HT29 tumors (*A*) and also in HUVEC on treatment with DA or the DA D_2 receptor agonist quinpirole (Quin) (*B*). (*C*) Pretreatment with the DA D_2 receptor antagonist eticlopride failed to inhibit ERK5 phosphorylation. Protein loading was verified by reblotting the membrane by anti-ERK5; total ERK5 expression remained unchanged. DA could not up-regulate KLF2 in ERK5-silenced HUVEC (siERK5). Results are representative of six separate experiments. NS, nonspecific control siRNA.